

The CKM suppressed $B(B_s) \rightarrow \bar{D}_{(s)}P, \bar{D}_{(s)}V, \bar{D}_{(s)}^*P, \bar{D}_{(s)}^*V$ decays in perturbative QCD approach

Hao Zou^a, Run-Hui Li^{a,b}, Xiao-Xia Wang^a, and Cai-Dian Lü^{a,c}

^a *Institute of High Energy Physics, P.O. Box 918(4), Beijing 100049, People's Republic of China*

^b *School of Physics, Shandong University, Jinan 250100, People's Republic of China*

^c *Theoretical Physics Center for Science Facilities, Beijing 100049, People's Republic of China*

(Dated: November 26, 2018)

Although the two-body charmed decays $B_{(s)} \rightarrow \bar{D}_{(s)}^{(*)}P$ and $\bar{D}_{(s)}^{(*)}V$, where $P(V)$ denotes a light pseudoscalar(vector) meson, are CKM suppressed comparing with the $B_{(s)} \rightarrow D_{(s)}^{(*)}P$ and $D_{(s)}^{(*)}V$ decays, they are important in the CKM angle $\gamma = \phi_3$ extraction method. We investigated these decays in the perturbative QCD approach to the leading order of m_D/m_B and Λ_{QCD}/m_D expansion. We find that the nonfactorizable emission diagrams and the annihilation diagrams are not negligible in many of these channels. The numerical results show that most channels have branching ratios with an order of 10^{-6} or 10^{-7} . The ratio needed for the CKM angle γ extraction is estimated as $r = \frac{|A(B^- \rightarrow \bar{D}^0 K^-)|}{|A(B^- \rightarrow \bar{D}^0 K^-)|} = 0.092^{+0.012+0.003}_{-0.003-0.003}$, which is too small for the experiments. Some of the $B_{(s)} \rightarrow \bar{D}_{(s)}^*V$ decays have a very large transversely polarized contribution that can reach 80%.

PACS: 13.25.Hw

I. INTRODUCTION

The study of B physics plays an important role in precise test of the standard model, extraction of the Cabibbo-Kobayashi-Maskawa(CKM) matrix elements, searching for the origin of CP violation and new physics signals and even discovery of new hadronic states. The hadronic B decays offer an opportunity to understand the nonperturbative QCD. After years of hard work, theorists develop many approaches to deal with the nonleptonic decays of B mesons, such as QCD factorization approach [1], soft collinear effective theory [2], perturbative QCD approach(PQCD)[3], QCD sum rules[4], light cone sum rules[5]. At the experimental side, the two B factories have accumulated a great amount of data, which can be used to either test various theoretical approaches or carry on new physics investigations.

The two body charmed decays of B mesons $B_{(s)} \rightarrow D_{(s)}^{(*)}P$ and $D_{(s)}^{(*)}V$, which are important in the extraction of the CKM angles [6], have been investigated in the PQCD approach [7, 8, 9]. These channels are induced by the $b \rightarrow c$ transitions, which are CKM favored. However, the method of CKM angle γ extraction [10] also requires another category of charmed meson B decays, which are induced by $b \rightarrow u$ transition. The interference between the $b \rightarrow c$ and $b \rightarrow u$ transitions gives the measurement of the CKM angle γ . These $b \rightarrow u$ decays are CKM $|V_{ub}/V_{cb}|$ suppressed, thus will have smaller branching ratios. In this paper, we will investigate these $B(B_s) \rightarrow \bar{D}_{(s)}P, \bar{D}_{(s)}V, \bar{D}_{(s)}^*P, \bar{D}_{(s)}^*V$ decays in the PQCD approach.

Unlike the collinear factorization in the QCD factorization approach and soft-collinear effective theory, the k_T factorization is utilized in the PQCD approach. In this approach, the transverse momentum of valence quarks in the mesons are kept to avoid the endpoint singularity. Therefore, only in this factorization method, one can calculate the color suppressed channels as well as the color allowed channels in charmed B decays. The conventional non-calculable

annihilation type decays are also calculable in the PQCD approach, which is proved to be the dominant strong phase in B decays for the direct CP asymmetry [11]. In the PQCD approach, the most important uncertainties come from the hadronic wave functions. We will use the same hadronic parameters determined from the charmed B decays induced by $b \rightarrow c$ transitions [9] to reduce uncertainties. The numerical results show that the $b \rightarrow u$ transition decays are indeed heavily suppressed comparing with those $b \rightarrow c$ transitions. Thus the CKM angle measurement method do face difficulty experimentally.

The paper is organized as follows: In Sec. II we list the analytic formulae needed in the calculation, including the Hamiltonian and definition of the momenta, PQCD factorization formulae of all the diagrams, and the expressions of the amplitudes for all the decay channels. Sec. III contains the numerical results we obtain, and some discussions. A brief summary is given in Sec. IV. The wave functions, decay constants and some functions that appear in PQCD approach are put in the appendices.

II. ANALYTIC FORMULAE FOR DECAY AMPLITUDES

In B meson weak decays, there are three natural energy scales involved: W boson mass, b quark mass scale and the hadronic scale Λ_{QCD} . The electroweak physics higher than W boson mass can be perturbatively calculated. The physics between b quark mass and W boson mass can also be calculated using the renormalization group equation. Both of these two contributions are included in the well calculated effective Hamiltonian of the four quark operators. The physics below b mass scale is complicated, where we have to utilize the factorization theorem to factorize the non-perturbative contribution out. In this purpose, we do the $1/m_b$ expansion in the soft collinear effective theory [2]. Unfortunately, there are some contributions, which produce endpoint singularity. In order to deal with this singularity, usually there are two ways of doing it. One of them is the PQCD approach, in which we keep the transverse momentum of the valence quark. By doing this k_T factorization, a new series of double logs are generated. Using the renormalization group equation, we resum these logs to give a Sudakov factor, which suppresses the endpoint contribution. Finally the decay amplitude becomes

$$\mathcal{M} = \int d^4k_1 d^4k_2 d^4k_3 \phi_B(k_1, t) T_H(k_1, k_2, k_3, t) \phi_{P_2}(k_2, t) \phi_{P_3}(k_3, t) e^{S(k_i, t)}, \quad (1)$$

where T_H is the hard part that is perturbatively calculable, and ϕ_M are the hadronic meson wave functions that is non-perturbative. The Sudakov factor $e^{S(k_i, t)}$ resulting from the resummation of double logarithm, relate the perturbative and non-perturbative dynamics.

In charmed B decays, we have one more intermediate energy scale, the D meson mass. Therefore, one encounters another expansion series of m_D/m_B . The factorization is only approved at the leading of m_D/m_B expansion [7, 8], so that we will keep only the leading order contribution numerically, unless explicitly mentioned.

A. Effective Hamiltonian and Kinematics

For the processes considered, only tree operators contribute, and the effective Hamiltonian is given by

$$\mathcal{H}_{eff} = \frac{G_F}{\sqrt{2}} V_{ub} V_{cd}^* [C_1(\mu) O_1(\mu) + C_2(\mu) O_2(\mu)], \quad (2)$$

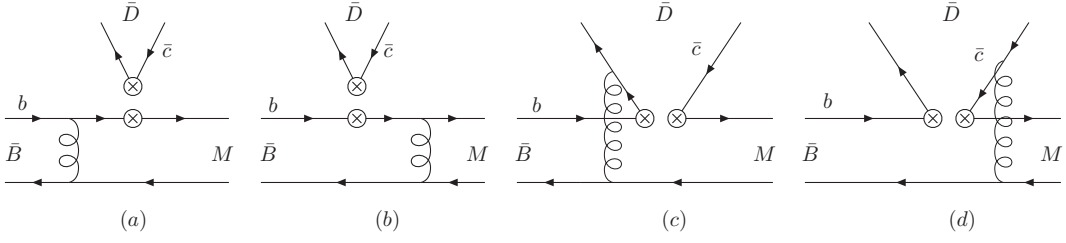


FIG. 1: Emission diagrams in pQCD approach for $B \rightarrow \bar{D}P$ decays.

with $D = d, s$, and

$$O_1 = (\bar{u}_\alpha b_\beta)_{V-A} (\bar{D}_\beta c_\alpha)_{V-A}, \quad O_2 = (\bar{u}_\alpha b_\alpha)_{V-A} (\bar{D}_\beta c_\beta)_{V-A}. \quad (3)$$

Here, α, β are the color indices, $(\bar{q}_1 q_2)_{V-A} \equiv \bar{q}_1 \gamma^\mu (1 - \gamma^5) q_2$. And the $V_{ub} V_{cD}^*$ are the corresponding CKM matrix elements.

Sandwiching the above Hamiltonian between the initial and final state mesons and factorizing the matrix elements, the combinations of the Wilson coefficients usually appear. Conventionally, they are defined as

$$a_1 = C_2 + C_1/3, \quad a_2 = C_1 + C_2/3, \quad (4)$$

where, a_1 and a_2 correspond to the color favored and color suppressed contribution, respectively. The light-cone coordinates are used in this paper, with which the vector V is expressed as $V = (\frac{V^0+V^3}{\sqrt{2}}, \frac{V^0-V^3}{\sqrt{2}}, V_\perp)$, where $V_\perp = (V^1, V^2)$. The momenta of B, D and the light mesons are respectively P_1, P_2 and P_3 , which are defined as

$$P_1 = \frac{m_B}{\sqrt{2}}(1, 1, \mathbf{0}_\perp), \quad P_2 = \frac{m_B}{\sqrt{2}}(1, r^2, \mathbf{0}_\perp), \quad P_3 = \frac{m_B}{\sqrt{2}}(0, 1 - r^2, \mathbf{0}_\perp), \quad (5)$$

with $r = m_D/m_B$. The momenta of the light quarks in B and D mesons are denoted by k_1 and k_2 , respectively, whereas k_3 represents the momentum of the quark in the light meson. Both k_1^+ and k_1^- contribute, but considering $k_2 \sim O(\Lambda)$ and $k_1 \sim O(x_1 m_B)$, we drop the term $k_1 \cdot k_1$ for the emission diagrams and $k_1 \cdot k_2$ for the annihilation diagrams. The effect is equal to dropping k_1^- for emission diagrams and dropping k_1^+ for annihilation diagrams. Their explicit expressions are

$$\begin{aligned} k_1 &= (x_1 \frac{m_B}{\sqrt{2}}, 0, \mathbf{k}_{1\perp}) \text{ for emission diagrams,} \\ k_1 &= (0, x_1 \frac{m_B}{\sqrt{2}}, \mathbf{k}_{1\perp}) \text{ for annihilation diagrams,} \\ k_2 &= (x_2 \frac{m_B}{\sqrt{2}}, 0, \mathbf{k}_{2\perp}), \quad k_3 = (0, x_3 \frac{(1-r^2)m_B}{\sqrt{2}}, \mathbf{k}_{3\perp}). \end{aligned} \quad (6)$$

Here, x_1, x_2 and x_3 are the momentum fractions, and $\mathbf{k}_{1\perp}, \mathbf{k}_{2\perp}$ and $\mathbf{k}_{3\perp}$ are the transverse momenta of the quarks.

B. Factorization formulae of $B \rightarrow \bar{D}P$

The contributions to the $B \rightarrow \bar{D}P$ processes can be divided into two types: The emission diagrams (see Fig. 1, denoted by a subscript *int* in the following formulae), in which the light quark in the B mesons is hadronized into

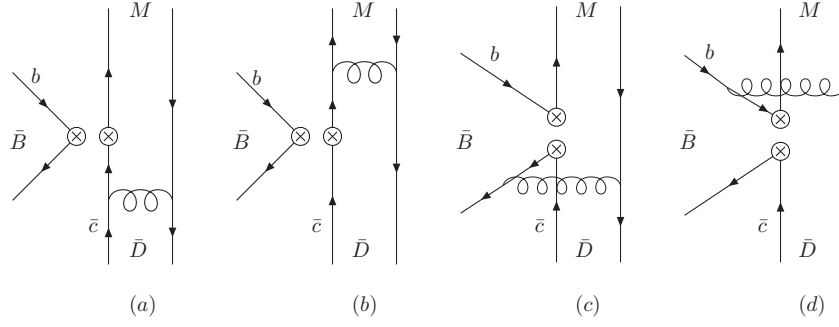


FIG. 2: Annihilation diagrams in pQCD approach for $B \rightarrow \bar{D}P$ decays.

one of the final state mesons as a spectator, and the annihilation diagrams (see Fig. 2, denoted by a subscript *exc* in the following formulae) with no spectator quarks. The first two diagrams of Fig. 1 are the factorizable diagrams, which can be factorized as a product of the decay constant of \bar{D} meson and a B to light meson transition form factor. Summing the expressions of these two diagrams together, we obtain

$$\begin{aligned} \xi_{\text{int}}(a_i) = & 8\pi C_F f_D \int_0^1 dx_1 dx_3 \int_0^{1/\Lambda} b_1 db_1 b_3 db_3 \phi_B(x_1, b_1) \\ & \times \{ [(2-x_3)\phi_P(x_3) - r_0(1-2x_3)(\phi_P^p(x_3) - \phi_P^T(x_3))] \\ & \times a_i(t_i^{(1)}) E_i(t_i^{(1)}) h_i(x_1, (1-x_3)(1-r^2), b_1, b_3) S_t(x_3) \\ & + 2r_0 \phi_P^p(x_3) a_i(t_i^{(2)}) E_i(t_i^{(2)}) h_i(1-x_3, x_1(1-r^2), b_3, b_1) S_t(x_1) \}, \end{aligned} \quad (7)$$

where a_i is the corresponding combination of Wilson coefficients and $r_0 = m_0/m_B$, with m_0 as the chiral mass of the pseudoscalar mesons. The expressions of the PQCD factorization functions h_j , jet function $S_t(x)$ and $E_j(t_j^l)$ and scales t_j^l , with $j = i, a, d, f$ and $l = 1$ or 2 , are listed in Appendix B.

In the factorized diagrams of annihilation contributions (the first two diagrams of Fig. 2), the B meson is factorized out. And the combination of these two diagrams give

$$\begin{aligned} \xi_{\text{exc}}(a_i) = & 8\pi C_F f_B \int_0^1 dx_2 dx_3 \int_0^{1/\Lambda} b_2 db_2 b_3 db_3 \phi_D(x_2, b_2) \\ & \times \left[(-x_2 \phi_P(x_3) - 2r_0 r (1+x_2) \phi_P^p(x_3)) a_i(t_a^{(1)}) E_a(t_a^{(1)}) h_a(1-x_3, x_2(1-r^2), b_3, b_2) S_t(x_3) \right. \\ & + ((1-x_3)\phi_P(x_3) + r_0 r ((2x_3-1)\phi_P^T(x_3) + (3-2x_3)\phi_P^p(x_3))) a_i(t_a^{(2)}) E_a(t_a^{(2)}) \\ & \left. \times h_a(x_2, (1-x_3)(1-r^2), b_2, b_3) S_t(x_2) \right]. \end{aligned} \quad (8)$$

The last two diagrams of Fig. 1 and 2 are nonfactorizable diagrams. Generally, if the two final state mesons are both light ones, the nonfactorizable contributions of the emission diagrams are very small, because of the cancelation between the two nonfactorizable diagrams. While for \bar{D} mesons, since the heavy \bar{c} quark and the light quark is not symmetric, the nonfactorizable emission diagrams give remarkable contributions. The expression of the nonfactorizable emission contributions is

$$\begin{aligned} \mathcal{M}_{\text{int}}(a_i) = & 16\pi \sqrt{2N_c} C_F \int_0^1 [dx] \int_0^{1/\Lambda} b_1 db_1 b_2 db_2 \phi_B(x_1, b_1) \phi_D(x_2, b_2) \\ & \times \left[(x_2 \phi_P(x_3) + r_0(x_3-1)(\phi_P^p(x_3) + \phi_P^T(x_3))) a_i(t_d^{(1)}) E_d(t_d^{(1)}) h_d^{(1)}(x_i, b_i) \right. \\ & \left. + ((x_3+x_2-2)\phi_P(x_3) + r_0(1-x_3)(\phi_P^p(x_3) - \phi_P^T(x_3))) a_i(t_d^{(2)}) E_d(t_d^{(2)}) h_d^{(2)}(x_i, b_i) \right], \end{aligned} \quad (9)$$

and that of the nonfactorizable annihilation contributions is

$$\begin{aligned}
\mathcal{M}_{\text{exc}}(a_i) &= 16\pi\sqrt{2N_c}C_F \int_0^1 [dx] \int_0^{1/\Lambda} b_1 db_1 b_2 db_2 \phi_B(x_1, b_1) \phi_D(x_2, b_2) \\
&\times [((x_3 - 1)\phi_P(x_3) - r_0 r((x_2 - x_3 + 3)\phi_P^p(x_3) + (x_2 + x_3 - 1)\phi_P^T(x_3)))a_i(t_f^{(1)})E_f(t_f^{(1)})h_f^{(1)}(x_i, b_i) \\
&+ (x_2\phi_P(x_3) - r_0 r((x_3 - x_2 - 1)\phi_P^p(x_3) + (x_2 + x_3 - 1)\phi_P^T(x_3)))a_i(t_f^{(2)})E_f(t_f^{(2)})h_f^{(2)}(x_i, b_i)]. \quad (10)
\end{aligned}$$

C. Amplitudes for $B \rightarrow \bar{D}P$

With the functions obtained in the above, the amplitudes of 22 $B \rightarrow \bar{D}P$ decay channels can be given by

$$\mathcal{A}(B^- \rightarrow \bar{D}^0 \pi^-) = \frac{G_F}{\sqrt{2}} m_B^4 V_{ub} V_{cd}^* (\xi_{int}(a_2) + \mathcal{M}_{int}(C_2/3) + \xi_{exc}(a_1) + \mathcal{M}_{exc}(C_1/3)), \quad (11)$$

$$\mathcal{A}(B^- \rightarrow \bar{D}^0 K^-) = \frac{G_F}{\sqrt{2}} m_B^4 V_{ub} V_{cs}^* (\xi_{int}(a_2) + \mathcal{M}_{int}(C_2/3) + \xi_{exc}(a_1) + \mathcal{M}_{exc}(C_1/3)), \quad (12)$$

$$\mathcal{A}(B^- \rightarrow D^- \pi^0) = \frac{G_F}{\sqrt{2}} m_B^4 V_{ub} V_{cd}^* \frac{1}{\sqrt{2}} (\xi_{int}(a_1) + \mathcal{M}_{int}(C_1/3) - \xi_{exc}(a_1) - \mathcal{M}_{exc}(C_1/3)), \quad (13)$$

$$\mathcal{A}(B^- \rightarrow D^- \bar{K}^0) = \frac{G_F}{\sqrt{2}} m_B^4 V_{ub} V_{cs}^* (\xi_{exc}(a_1) + \mathcal{M}_{exc}(C_1/3)), \quad (14)$$

$$\mathcal{A}(B^- \rightarrow D^- \eta_{m\bar{n}}) = \frac{G_F}{\sqrt{2}} m_B^4 V_{ub} V_{cd}^* \frac{1}{\sqrt{2}} (\xi_{int}(a_1) + \mathcal{M}_{int}(C_1/3) + \xi_{exc}(a_1) + \mathcal{M}_{exc}(C_1/3)), \quad (15)$$

$$\mathcal{A}(B^- \rightarrow D_s^- \pi^0) = \frac{G_F}{\sqrt{2}} m_B^4 V_{ub} V_{cs}^* \frac{1}{\sqrt{2}} (\xi_{int}(a_1) + \mathcal{M}_{int}(C_1/3)), \quad (16)$$

$$\mathcal{A}(B^- \rightarrow D_s^- K^0) = \frac{G_F}{\sqrt{2}} m_B^4 V_{ub} V_{cd}^* (\xi_{exc}(a_1) + \mathcal{M}_{exc}(C_1/3)), \quad (17)$$

$$\mathcal{A}(B^- \rightarrow D_s^- \eta_{m\bar{n}}) = \frac{G_F}{\sqrt{2}} m_B^4 V_{ub} V_{cs}^* \frac{1}{\sqrt{2}} (\xi_{int}(a_1) + \mathcal{M}_{int}(C_1/3)), \quad (18)$$

$$\mathcal{A}(B^- \rightarrow D_s^- \eta_{s\bar{s}}) = \frac{G_F}{\sqrt{2}} m_B^4 V_{ub} V_{cs}^* (\xi_{exc}(a_1) + \mathcal{M}_{exc}(C_1/3)), \quad (19)$$

$$\mathcal{A}(\bar{B}^0 \rightarrow \bar{D}^0 \pi^0) = \frac{G_F}{\sqrt{2}} m_B^4 V_{ub} V_{cd}^* \frac{1}{\sqrt{2}} (-\xi_{int}(a_2) - \mathcal{M}_{int}(C_2/3) + \xi_{exc}(a_2) + \mathcal{M}_{exc}(C_2/3)), \quad (20)$$

$$\mathcal{A}(\bar{B}^0 \rightarrow \bar{D}^0 \bar{K}^0) = \frac{G_F}{\sqrt{2}} m_B^4 V_{ub} V_{cs}^* (\xi_{int}(a_2) + \mathcal{M}_{int}(C_2/3)), \quad (21)$$

$$\mathcal{A}(\bar{B}^0 \rightarrow \bar{D}^0 \eta_{m\bar{n}}) = \frac{G_F}{\sqrt{2}} m_B^4 V_{ub} V_{cd}^* \frac{1}{\sqrt{2}} (\xi_{int}(a_2) + \mathcal{M}_{int}(C_2/3) + \xi_{exc}(a_2) + \mathcal{M}_{exc}(C_2/3)), \quad (22)$$

$$\mathcal{A}(\bar{B}^0 \rightarrow D^- \pi^+) = \frac{G_F}{\sqrt{2}} m_B^4 V_{ub} V_{cd}^* (\xi_{int}(a_1) + \mathcal{M}_{int}(C_1/3) + \xi_{exc}(a_2) + \mathcal{M}_{exc}(C_2/3)), \quad (23)$$

$$\mathcal{A}(\bar{B}^0 \rightarrow D_s^- \pi^+) = \frac{G_F}{\sqrt{2}} m_B^4 V_{ub} V_{cs}^* (\xi_{int}(a_1) + \mathcal{M}_{int}(C_1/3)), \quad (24)$$

$$\mathcal{A}(\bar{B}^0 \rightarrow D_s^- K^+) = \frac{G_F}{\sqrt{2}} m_B^4 V_{ub} V_{cd}^* (\xi_{exc}(a_2) + \mathcal{M}_{exc}(C_2/3)), \quad (25)$$

$$\mathcal{A}(\bar{B}_s^0 \rightarrow \bar{D}^0 \pi^0) = \frac{G_F}{\sqrt{2}} m_B^4 V_{ub} V_{cs}^* \frac{1}{\sqrt{2}} (\xi_{exc}(a_2) + \mathcal{M}_{exc}(C_2/3)), \quad (26)$$

$$\mathcal{A}(\bar{B}_s^0 \rightarrow \bar{D}^0 K^0) = \frac{G_F}{\sqrt{2}} m_B^4 V_{ub} V_{cd}^* (\xi_{int}(a_2) + \mathcal{M}_{int}(C_2/3)), \quad (27)$$

$$\mathcal{A}(\bar{B}_s^0 \rightarrow \bar{D}^0 \eta_{m\bar{n}}) = \frac{G_F}{\sqrt{2}} m_B^4 V_{ub} V_{cs}^* \frac{1}{\sqrt{2}} (\xi_{exc}(a_2) + \mathcal{M}_{exc}(C_2/3)), \quad (28)$$

$$\mathcal{A}(\bar{B}_s^0 \rightarrow \bar{D}^0 \eta_{s\bar{s}}) = \frac{G_F}{\sqrt{2}} m_B^4 V_{ub} V_{cs}^* (\xi_{int}(a_2) + \mathcal{M}_{int}(C_2/3)), \quad (29)$$

$$\mathcal{A}(\bar{B}_s^0 \rightarrow D^- \pi^+) = \frac{G_F}{\sqrt{2}} m_B^4 V_{ub} V_{cs}^* (\xi_{exc}(a_2) + \mathcal{M}_{exc}(C_2/3)), \quad (30)$$

$$\mathcal{A}(\bar{B}_s^0 \rightarrow D^- K^+) = \frac{G_F}{\sqrt{2}} m_B^4 V_{ub} V_{cd}^* (\xi_{int}(a_1) + \mathcal{M}_{int}(C_1/3)), \quad (31)$$

$$\mathcal{A}(\bar{B}_s^0 \rightarrow D_s^- K^+) = \frac{G_F}{\sqrt{2}} m_B^4 V_{ub} V_{cs}^* (\xi_{int}(a_1) + \mathcal{M}_{int}(C_1/3) + \xi_{exc}(a_2) + \mathcal{M}_{exc}(C_2/3)), \quad (32)$$

where $\eta_{m\bar{n}} = \frac{1}{\sqrt{2}}(u\bar{u} + d\bar{d})$ and $\eta_{s\bar{s}} = s\bar{s}$. We treat η and η' as the mixtures of $\eta_{m\bar{n}}$ and $\eta_{s\bar{s}}$ with

$$\begin{pmatrix} \eta \\ \eta' \end{pmatrix} = \begin{pmatrix} \cos \phi & -\sin \phi \\ \sin \phi & \cos \phi \end{pmatrix} \begin{pmatrix} \eta_{m\bar{n}} \\ \eta_{s\bar{s}} \end{pmatrix}, \quad (33)$$

where $\phi = 39.3^\circ \pm 1.0^\circ$ [12].

D. Decay Amplitudes for $B \rightarrow \bar{D}^*P$ and $B \rightarrow \bar{D}^{(*)}V$ modes

Due to the conservation of the angular momentum, only the longitudinally polarized vector mesons are generated in the $B \rightarrow \bar{D}V$ and $B \rightarrow \bar{D}^*P$ decay modes. According to the similarity between the Lorentz structures of the wave functions for the pseudoscalar mesons and vector mesons, the emission diagrams' factorization formulae of $B \rightarrow \bar{D}V$ modes can be obtained by making the following substitutions in Eq. (7) and (9) up to the leading order and leading power of $1/m_B$:

$$\phi_P \rightarrow \phi_V, \quad \phi_P^p \rightarrow -\phi_V^s, \quad \phi_P^T \rightarrow -\phi_V^t, \quad r_0 \rightarrow r_V, \quad f_P \rightarrow f_V. \quad (34)$$

The factorization formula for the annihilation diagrams of $B \rightarrow \bar{D}V$ decays are listed below:

$$\begin{aligned} \xi_{\text{exc}}(a_i) &= 8\pi C_F f_B \int_0^1 dx_2 dx_3 \int_0^{1/\Lambda} b_2 db_2 b_3 db_3 \phi_D(x_2, b_2) \\ &\times \left[(-x_2 \phi_V(x_3) + 2r_V r(1+x_2) \phi_V^s(x_3)) a_i(t_a^{(1)}) E_a(t_a^{(1)}) h_a(1-x_3, x_2(1-r^2), b_3, b_2) S_t(x_3) \right. \\ &+ ((1-x_3) \phi_V(x_3) + r_V r((1-2x_3) \phi_V^t(x_3) - (3-2x_3) \phi_V^s(x_3))) a_i(t_a^{(2)}) E_a(t_a^{(2)}) \\ &\left. \times h_a(x_2, (1-x_3)(1-r^2), b_2, b_3) S_t(x_2) \right]. \quad (35) \end{aligned}$$

$$\begin{aligned} \mathcal{M}_{\text{exc}}(a_i) &= 16\pi \sqrt{2N_c} C_F \int_0^1 [dx] \int_0^{1/\Lambda} b_1 db_1 b_2 db_2 \phi_B(x_1, b_1) \phi_D(x_2, b_2) \\ &\times [((x_3-1) \phi_V(x_3) + r_V r((x_2+x_3-1) \phi_V^t(x_3) + (x_2-x_3+3) \phi_V^s(x_3))) a_i(t_f^{(1)}) E_f(t_f^{(1)}) h_f^{(1)}(x_i, b_i) \\ &+ (x_2 \phi_V(x_3) - r_V r((x_2-x_3+1) \phi_V^s(x_3) - (x_2+x_3-1) \phi_V^t(x_3))) a_i(t_f^{(2)}) E_f(t_f^{(2)}) h_f^{(2)}(x_i, b_i)]. \quad (36) \end{aligned}$$

By changing the pseudoscalar nonet to corresponding vector nonet in Eq.(11)-(32), one will obtain the decay amplitudes formula for the corresponding $B \rightarrow \bar{D}V$ mode.

While in order to obtain the factorization formulae for $B \rightarrow \bar{D}^*P$ mode, the substitutions

$$\phi_D \rightarrow \phi_D^L, \quad f_D \rightarrow f_{D^*}, \quad m_D \rightarrow m_{D^*} \quad (37)$$

should be made in Eq.(7) and (9) for emission diagrams. The annihilation diagrams' formulae are listed below:

$$\begin{aligned} \xi_{\text{exc}}(a_i) &= 8\pi C_F f_B \int_0^1 dx_2 dx_3 \int_0^{1/\Lambda} b_2 db_2 b_3 db_3 \phi_D(x_2, b_2) \\ &\times \left[(-x_2 \phi_P(x_3) + 2r_0 r(1-x_2) \phi_P^p(x_3)) a_i(t_a^{(1)}) E_a(t_a^{(1)}) h_a(1-x_3, x_2(1-r^2), b_3, b_2) S_t(x_3) \right. \\ &\left. + ((1-x_3) \phi_P(x_3) + r_0 r(\phi_P^T(x_3) + \phi_P^p(x_3))) a_i(t_a^{(2)}) E_a(t_a^{(2)}) h_a(x_2, (1-x_3)(1-r^2), b_2, b_3) S_t(x_2) \right] \quad (38) \end{aligned}$$

$$\begin{aligned} \mathcal{M}_{\text{exc}}(a_i) &= 16\pi \sqrt{2N_c} C_F \int_0^1 [dx] \int_0^{1/\Lambda} b_1 db_1 b_2 db_2 \phi_B(x_1, b_1) \phi_D(x_2, b_2) \\ &\times [((x_3-1) \phi_P(x_3) - r_0 r((1-x_2-x_3) \phi_P^p(x_3) + (1-x_2+x_3) \phi_P^T(x_3))) a_i(t_f^{(1)}) E_f(t_f^{(1)}) h_f^{(1)}(x_i, b_i) \\ &+ (x_2 \phi_P(x_3) + r_0 r((x_3-x_2-1) \phi_P^T(x_3) + (x_2+x_3-1) \phi_P^p(x_3))) a_i(t_f^{(2)}) E_f(t_f^{(2)}) h_f^{(2)}(x_i, b_i)]. \quad (39) \end{aligned}$$

The decay amplitudes for these modes can be got through changing the \bar{D} mesons to corresponding \bar{D}^* mesons in (11)-(32).

The situation for $B \rightarrow \bar{D}^*V$ mode is a little more complicated. Both the longitudinal polarization and the transverse polarization contribute. The longitudinally polarized factorization formulae are obtained by making the following substitutions in Eq. (7) and (9):

$$\phi_P \rightarrow -\phi_V, \phi_P^p \rightarrow \phi_V^s, \phi_P^T \rightarrow \phi_V^t, r_0 \rightarrow r_V, f_P \rightarrow f_V, \phi_D \rightarrow \phi_D^L, f_D \rightarrow f_{D^*}, m_D \rightarrow m_{D^*}. \quad (40)$$

The annihilation diagrams' formula are

$$\begin{aligned} \xi_{\text{exc}}(a_i) = & -8\pi C_F f_B \int_0^1 dx_2 dx_3 \int_0^{1/\Lambda} b_2 db_2 b_3 db_3 \phi_D(x_2, b_2) \\ & \times \left[(-x_2 \phi_V(x_3) + 2r_V r(x_2 - 1) \phi_V^s(x_3)) a_i(t_a^{(1)}) E_a(t_a^{(1)}) h_a(1 - x_3, x_2(1 - r^2), b_3, b_2) S_t(x_3) \right. \\ & \left. + ((1 - x_3) \phi_V(x_3) - r_V r(\phi_V^t(x_3) + \phi_V^s(x_3))) a_i(t_a^{(2)}) E_a(t_a^{(2)}) h_a(x_2, (1 - x_3)(1 - r^2), b_2, b_3) S_t(x_2) \right] \end{aligned} \quad (41)$$

$$\begin{aligned} \mathcal{M}_{\text{exc}}(a_i) = & -16\pi \sqrt{2N_c} C_F \int_0^1 [dx] \int_0^{1/\Lambda} b_1 db_1 b_2 db_2 \phi_B(x_1, b_1) \phi_D(x_2, b_2) \\ & \times [((x_3 - 1) \phi_V(x_3) - r_V r((x_2 - x_3 - 1) \phi_V^t(x_3) + (x_2 + x_3 - 1) \phi_V^s(x_3))) a_i(t_f^{(1)}) E_f(t_f^{(1)}) h_f^{(1)}(x_i, b_i) \\ & + (x_2 \phi_V(x_3) + r_V r((1 - x_2 - x_3) \phi_V^s(x_3) + (x_2 - x_3 + 1) \phi_V^t(x_3))) a_i(t_f^{(2)}) E_f(t_f^{(2)}) h_f^{(2)}(x_i, b_i)]. \end{aligned} \quad (42)$$

The longitudinally polarized decay amplitudes \mathcal{A}^N s can be obtained through replacing the pseudo-scalar mesons by the corresponding light vector mesons and the \bar{D}^* meson in (11)-(32).

The transversely polarized amplitude of $B \rightarrow \bar{D}^*V$ mode can be decomposed as

$$\mathcal{A}^T(\epsilon_D^{T*}, \epsilon_V^{T*}) = \frac{G_F}{\sqrt{2}} m_B^4 V_{ub} V_{cd}^* \left[i(\epsilon_D^{T*} \cdot \epsilon_V^{T*}) A^s + \epsilon^{\mu\nu\rho\sigma} n_\mu \bar{n}_\nu \epsilon_{D,\rho}^{T*} \epsilon_{V,\sigma}^{T*} A^p \right], \quad (43)$$

where $\mathcal{A}^{s/p} = \xi_{\text{int}}^{s/p} + \mathcal{M}_{\text{int}}^{s/p} + \xi_{\text{exc}}^{s/p} + \mathcal{M}_{\text{exc}}^{s/p}$. $\xi_{\text{int}}^{s/p}$, $\mathcal{M}_{\text{int}}^{s/p}$, $\xi_{\text{exc}}^{s/p}$, $\mathcal{M}_{\text{exc}}^{s/p}$ correspond to the factorizable emission diagrams, nonfactorizable diagrams, factorizable annihilation diagrams and nonfactorizable diagrams respectively, and their analytic expressions are given in Eq.(44)-Eq.(51). ϵ_D^T and ϵ_V^T are the respective transverse polarization vectors of \bar{D}^* and vector mesons, \bar{n} is the light cone vector in which direction the momentum of the vector meson is defined and n is the opposite direction. $\epsilon^{\mu\nu\rho\sigma}$ is the antisymmetric tensor with $\epsilon^{0123} = 1$.

The transversely polarized contributions are suppressed by r or r_V , and their expressions are given by

$$\begin{aligned} \xi_{\text{int}}^s(a_i) = & 8\pi C_F f_{D^*} r \int_0^1 dx_1 dx_3 \int_0^{1/\Lambda} b_1 db_1 b_3 db_3 \phi_B(x_1, b_1) \\ & \times \{ [-\phi_V^T(x_3) + r_V ((x_3 - 1) \phi_V^a(x_3) + (x_3 - 3) \phi_V^v)] \\ & \times a_i(t_i^{(1)}) E_i(t_i^{(1)}) h(x_1, (1 - x_3)(1 - r^2), b_1, b_3) S_t(x_3) \\ & + r_V [\phi_V^a(x_3) - \phi_V^v(x_3)] a_i(t_i^{(2)}) E_i(t_i^{(2)}) h(1 - x_3, x_1(1 - r^2), b_3, b_1) S_t(x_1) \}, \end{aligned} \quad (44)$$

$$\begin{aligned} \xi_{\text{int}}^p(a_i) = & 8\pi C_F f_{D^*} r \int_0^1 dx_1 dx_3 \int_0^{1/\Lambda} b_1 db_1 b_3 db_3 \phi_B(x_1, b_1) \\ & \times \{ [-\phi_V^T(x_3) - r_V ((x_3 - 1) \phi_V^v(x_3) + (x_3 - 3) \phi_V^a)] \\ & \times a_i(t_i^{(1)}) E_i(t_i^{(1)}) h(x_1, (1 - x_3)(1 - r^2), b_1, b_3) S_t(x_3) \\ & + r_V [\phi_V^a(x_3) - \phi_V^v(x_3)] a_i(t_i^{(2)}) E_i(t_i^{(2)}) h(1 - x_3, x_1(1 - r^2), b_3, b_1) S_t(x_1) \}, \end{aligned} \quad (45)$$

$$\begin{aligned}
\mathcal{M}_{\text{int}}^s(a_i) &= 16\pi\sqrt{2N_c}C_{Fr} \int_0^1 [dx] \int_0^{1/\Lambda} b_1 db_1 b_2 db_2 \phi_B(x_1, b_1) \phi_D^T(x_2, b_2) \\
&\times \left[-x_2 \phi_V^T(x_3) a_i(t_d^{(1)}) E_d(t_d^{(1)}) h_d^{(1)}(x_i, b_i) \right. \\
&\left. + (-r_V(\phi_V^a(x_3) + (2x_2 + 2x_3 - 5)\phi_V^v(x_3)) + (x_2 - 3)\phi_V^T(x_3)) a_i(t_d^{(2)}) E_d(t_d^{(2)}) h_d^{(2)}(x_i, b_i) \right], \quad (46)
\end{aligned}$$

$$\begin{aligned}
\mathcal{M}_{\text{int}}^p(a_i) &= 16\pi\sqrt{2N_c}C_{Fr} \int_0^1 [dx] \int_0^{1/\Lambda} b_1 db_1 b_2 db_2 \phi_B(x_1, b_1) \phi_D^T(x_2, b_2) \\
&\times \left[-x_2 \phi_V^T(x_3) a_i(t_d^{(1)}) E_d(t_d^{(1)}) h_d^{(1)}(x_i, b_i) \right. \\
&\left. + (r_V(\phi_V^v(x_3) + (2x_2 + 2x_3 - 5)\phi_V^a(x_3)) + (x_2 - 3)\phi_V^T(x_3)) a_i(t_d^{(2)}) E_d(t_d^{(2)}) h_d^{(2)}(x_i, b_i) \right], \quad (47)
\end{aligned}$$

$$\begin{aligned}
\xi_{\text{exc}}^s(a_i) &= 8\pi C_F f_B \int_0^1 dx_2 dx_3 \int_0^{1/\Lambda} b_2 db_2 b_3 db_3 \phi_D^T(x_2, b_2) \\
&\times \left[rr_V \left((x_2 - 1)\phi_V^a(x_3) + (x_2 + 1)\phi_V^v(x_3) \right) a_i(t_a^{(1)}) E_a(t_a^{(1)}) h_a(1 - x_3, x_2(1 - r^2), b_3, b_2) S_t(x_3) \right. \\
&\left. + \left(rr_V(x_3(\phi_V^v(x_3) - \phi_V^a(x_3)) - 2\phi_V^v(x_3)) + r^2 \phi_V^T(x_3) \right) \right. \\
&\left. \times a_i(t_a^{(2)}) E_a(t_a^{(2)}) h_a(x_2, (1 - x_3)(1 - r^2), b_2, b_3) S_t(x_2) \right], \quad (48)
\end{aligned}$$

$$\begin{aligned}
\xi_{\text{exc}}^p(a_i) &= 8\pi C_F f_B \int_0^1 dx_2 dx_3 \int_0^{1/\Lambda} b_2 db_2 b_3 db_3 \phi_D^T(x_2, b_2) \\
&\times \left[-rr_V \left((x_2 - 1)\phi_V^v(x_3) + (x_2 + 1)\phi_V^a(x_3) \right) a_i(t_a^{(1)}) E_a(t_a^{(1)}) h_a(1 - x_3, x_2(1 - r^2), b_3, b_2) S_t(x_3) \right. \\
&\left. + \left(rr_V(x_3(\phi_V^v(x_3) - \phi_V^a(x_3)) + 2\phi_V^a(x_3)) + r^2 \phi_V^T(x_3) \right) \right. \\
&\left. \times a_i(t_a^{(2)}) E_a(t_a^{(2)}) h_a(x_2, (1 - x_3)(1 - r^2), b_2, b_3) S_t(x_2) \right], \quad (49)
\end{aligned}$$

$$\begin{aligned}
\mathcal{M}_{\text{exc}}^s(a_i) &= 16\pi\sqrt{2N_c}C_F \int_0^1 [dx] \int_0^{1/\Lambda} b_1 db_1 b_2 db_2 \phi_B(x_1, b_1) \phi_D^T(x_2, b_2) \\
&\times [2rr_V \phi_V^v(x_3) a_i(t_f^{(1)}) E_f(t_f^{(1)}) h_f^{(1)}(x_i, b_i) \\
&+ (-x_2 r^2 \phi_V^T(x_3)) a_i(t_f^{(2)}) E_f(t_f^{(2)}) h_f^{(2)}(x_i, b_i)]. \quad (50)
\end{aligned}$$

$$\begin{aligned}
\mathcal{M}_{\text{exc}}^p(a_i) &= 16\pi\sqrt{2N_c}C_F \int_0^1 [dx] \int_0^{1/\Lambda} b_1 db_1 b_2 db_2 \phi_B(x_1, b_1) \phi_D^T(x_2, b_2) \\
&\times [(-2rr_V \phi_V^a(x_3) a_i(t_f^{(1)}) E_f(t_f^{(1)}) h_f^{(1)}(x_i, b_i) \\
&+ (-x_2 r^2 \phi_V^T(x_3)) a_i(t_f^{(2)}) E_f(t_f^{(2)}) h_f^{(2)}(x_i, b_i)]. \quad (51)
\end{aligned}$$

III. NUMERICAL RESULTS AND DISCUSSIONS

Although the meson wave functions are not perturbatively calculable, they are universal for all the decay channels. We can determine them from the well measured decay channels, such as the $B \rightarrow D^{(*)}P$ decays [9]. We use the same light cone distribution amplitudes as those we obtained in Ref. [9]. The Lorentz structure of wave functions,

TABLE I: Branching ratios of $B_{(s)} \rightarrow \bar{D}P$ decays calculated in PQCD approach together with experimental data[13] (unit: 10^{-6}).

Modes	class	Experiments	Our results
$\bar{B}^0 \rightarrow D_s^- \pi^+$	T	15.3 ± 3.5	$33.0^{+17.4+1.9+3.2}_{-12.6-1.8-3.1}$
$\bar{B}^0 \rightarrow D_s^- K^+$	E		$(0.47^{+0.14+0.08+0.05}_{-0.15-0.12-0.04}) \times 10^{-2}$
$\bar{B}^0 \rightarrow \bar{D}^0 \pi^0$	C		$(4.50^{+2.3+1.5+0.44}_{-1.6-1.2-0.41}) \times 10^{-2}$
$\bar{B}^0 \rightarrow \bar{D}^0 \bar{K}^0$	C		$1.79^{+0.95+0.78+0.18}_{-0.74-0.55-0.17}$
$\bar{B}^0 \rightarrow \bar{D}^0 \eta$	C		$(6.16^{+3.1+1.5+0.61}_{-2.3-1.3-0.57}) \times 10^{-2}$
$\bar{B}^0 \rightarrow \bar{D}^0 \eta'$	C		$(4.12^{+2.1+1.0+0.41}_{-1.5-0.90-0.38}) \times 10^{-2}$
$\bar{B}^0 \rightarrow D^- \pi^+$	T		$1.10^{+0.58+0.07+0.11}_{-0.43-0.07-0.10}$
$B^- \rightarrow \bar{D}^0 \pi^-$	C		$0.17^{+0.07+0.03+0.02}_{-0.06-0.03-0.02}$
$B^- \rightarrow \bar{D}^0 K^-$	C		$2.89^{+1.45+1.32+0.28}_{-0.95-0.81-0.27}$
$B^- \rightarrow D^- \pi^0$	T		$0.75^{+0.35+0.05+0.07}_{-0.27-0.06-0.07}$
$B^- \rightarrow D^- \bar{K}^0$	A	< 5.0	$0.19^{+0.06+0.19+0.02}_{-0.06-0.16-0.02}$
$B^- \rightarrow D^- \eta$	T		$0.37^{+0.19+0.03+0.04}_{-0.14-0.03-0.03}$
$B^- \rightarrow D^- \eta'$	T		$0.24^{+0.13+0.02+0.02}_{-0.10-0.02-0.02}$
$B^- \rightarrow D_s^- \pi^0$	T		$17.9^{+9.4+1.0+1.8}_{-6.8-1.01-1.7}$
$B^- \rightarrow D_s^- K^0$	A		$(0.68^{+0.39+0.90+0.07}_{-0.10-0.45-0.06}) \times 10^{-2}$
$B^- \rightarrow D_s^- \eta$	T		$10.3^{+4.8+0.57+1.0}_{-3.7-1.4-0.96}$
$B^- \rightarrow D_s^- \eta'$	T		$5.71^{+3.41+0.73+0.56}_{-2.28-0.46-0.53}$
$\bar{B}_s^0 \rightarrow \bar{D}^0 \pi^0$	E		$(9.54^{+3.5+0.30+0.93}_{-3.4-1.7-0.89}) \times 10^{-2}$
$\bar{B}_s^0 \rightarrow \bar{D}^0 K^0$	C		$(2.43^{+1.4+1.6+0.24}_{-1.0-0.98-0.23}) \times 10^{-2}$
$\bar{B}_s^0 \rightarrow \bar{D}^0 \eta$	C		$1.10^{+0.50+0.25+0.11}_{-0.41-0.26-0.10}$
$\bar{B}_s^0 \rightarrow \bar{D}^0 \eta'$	C		$2.58^{+1.2+0.59+0.25}_{-0.94-0.54-0.24}$
$\bar{B}_s^0 \rightarrow D^- \pi^+$	E		$0.19^{+0.07+0.01+0.01}_{-0.06-0.03-0.01}$
$\bar{B}_s^0 \rightarrow D^- K^+$	T		$1.21^{+0.58+0.10+0.12}_{-0.43-0.13-0.11}$
$\bar{B}_s^0 \rightarrow D_s^- K^+$	T		$29.4^{+14.3+2.7+2.9}_{-10.6-3.5-2.7}$

decay constants, and some parameters of PQCD approach, are listed in the appendix A. With the formulae we list in Sec. II, we can get the amplitude \mathcal{A} for each channel. The decay width for the $B_{(s)} \rightarrow \bar{D}_{(s)}^* V$ mode is given by

$$\begin{aligned}
\Gamma &= \frac{1}{16\pi m_B} (1 - r^2) \sum_{\epsilon_D, \epsilon_V} |\mathcal{A}^X|^2 \quad (X = N, T) \\
&= \frac{1}{16\pi m_B} (1 - r^2) (|\mathcal{A}^N|^2 + 2(|\mathcal{A}^s|^2 + |\mathcal{A}^p|^2)).
\end{aligned} \tag{52}$$

For the other three kinds of decay modes $B \rightarrow \bar{D}_{(s)}^{(*)} P$ and $B \rightarrow \bar{D}_{(s)} V$, the decay width is given by

$$\Gamma = \frac{1}{16\pi m_B} (1 - r^2) |\mathcal{A}|^2. \tag{53}$$

With the decay width at hand, the branching ratio is given by $\mathcal{BR} = \Gamma \tau_B$. We take $\tau_{B^-} = (1.674 \times 10^{-12})s/\hbar$, $\tau_{\bar{B}^0} = (1.542 \times 10^{-12})s/\hbar$, $\tau_{\bar{B}_s^0} = (1.466 \times 10^{-12})s/\hbar$, and $G_F = 1.16639 \times 10^{-5} \text{GeV}^{-2}$ [13]. Our numerical results

TABLE II: Branching ratios of $B_{(s)} \rightarrow \bar{D}V$ decays calculated in PQCD approach together with experimental data[13] (unit: 10^{-6}).

Modes	Class	Experiments	Our results
$\bar{B}^0 \rightarrow D_s^- \rho^+$	T	< 600	$35.9^{+17.8+2.0+3.5}_{-13.2-1.9-3.3}$
$\bar{B}^0 \rightarrow D_s^- K^{*+}$	E		$(1.68^{+0.63+0.42+0.16}_{-0.43-0.31-0.15}) \times 10^{-2}$
$\bar{B}^0 \rightarrow \bar{D}^0 \rho^0$	C		$(3.44^{+1.8+1.2+0.34}_{-1.3-0.78-0.32}) \times 10^{-2}$
$\bar{B}^0 \rightarrow \bar{D}^0 \bar{K}^{*0}$	C	< 11.0	$1.92^{+0.95+0.75+0.18}_{-0.77-0.52-0.17}$
$\bar{B}^0 \rightarrow \bar{D}^0 \omega$	C		$(6.13^{+2.7+1.6+0.59}_{-2.2-1.1-0.57}) \times 10^{-2}$
$\bar{B}^0 \rightarrow D^- \rho^+$	T		$1.27^{+0.65+0.07+0.12}_{-0.48-0.06-0.12}$
$B^- \rightarrow \bar{D}^0 \rho^-$	C		$(9.27^{+4.6+3.5+0.91}_{-3.5-2.1-0.9}) \times 10^{-2}$
$B^- \rightarrow \bar{D}^0 K^{*-}$	C		$2.05^{+1.1+0.94+0.20}_{-0.76-0.49-0.19}$
$B^- \rightarrow D^- \rho^0$	T		$0.75^{+0.37+0.05+0.07}_{-0.28-0.05-0.07}$
$B^- \rightarrow D^- \bar{K}^{*0}$	A		$0.11^{+0.03+0.01+0.01}_{-0.04-0.02-0.01}$
$B^- \rightarrow D^- \omega$	T		$0.67^{+0.32+0.03+0.06}_{-0.25-0.04-0.06}$
$B^- \rightarrow D_s^- \rho^0$	T		$19.4^{+9.5+1.0+1.9}_{-7.2-1.1-1.8}$
$B^- \rightarrow D_s^- K^{*0}$	A		$(0.50^{+0.16+0.14+0.05}_{-0.15-0.14-0.05}) \times 10^{-2}$
$B^- \rightarrow D_s^- \omega$	T		$16.8^{+8.3+0.94+1.6}_{-6.2-0.93-1.6}$
$B^- \rightarrow D_s^- \phi$	A	< 1.90	$0.13^{+0.05+0.03+0.02}_{-0.04-0.02-0.02}$
$\bar{B}_s^0 \rightarrow \bar{D}^0 \rho^0$	E		$0.19^{+0.05+0.04+0.02}_{-0.05-0.03-0.02}$
$\bar{B}_s^0 \rightarrow \bar{D}^0 K^{*0}$	C		$(0.60^{+0.32+0.27+0.06}_{-0.22-0.17-0.06}) \times 10^{-2}$
$\bar{B}_s^0 \rightarrow \bar{D}^0 \omega$	E		$0.16^{+0.05+0.02+0.01}_{-0.05-0.03-0.01}$
$\bar{B}_s^0 \rightarrow \bar{D}^0 \phi$	C		$1.89^{+1.0+0.71+0.18}_{-0.69-0.45-0.18}$
$\bar{B}_s^0 \rightarrow D^- \rho^+$	E		$0.37^{+0.11+0.06+0.04}_{-0.10-0.07-0.03}$
$\bar{B}_s^0 \rightarrow D^- K^{*+}$	T		$1.42^{+0.63+0.08+0.14}_{-0.48-0.12-0.13}$
$\bar{B}_s^0 \rightarrow D_s^- K^{*+}$	T		$33.1^{+15.4+1.63+3.06}_{-11.6-2.65-3.07}$

are listed in Table I, II, III and IV. The first error is from the hadronic parameters of $B_{(s)}$ meson wave functions(the decay constants and the shape parameters): $f_B = (0.19 \pm 0.025)\text{GeV}$, $f_{B_s} = (0.24 \pm 0.03)\text{GeV}$, $\omega_b = (0.40 \pm 0.05)\text{GeV}$ for B meson, and $\omega_b = (0.50 \pm 0.05)\text{GeV}$ for B_s meson. The second error arises from the choice of the hard scales, which vary from $0.75t$ to $1.25t$, and the uncertainty of $\Lambda_{QCD} = (0.25 \pm 0.05)\text{GeV}$. This uncertainty characterize the size of the next-to-leading order QCD corrections, which is shown reasonable in these tables. The third error comes from the uncertainties of the CKM matrix elements:

$$\begin{aligned}
|V_{ub}| &= 0.003\ 59 \pm 0.000\ 16, & |V_{cd}| &= 0.225\ 6 \pm 0.001\ 0, \\
|V_{cs}| &= 0.973\ 34 \pm 0.000\ 23, & \gamma &= (77^{+30}_{-32})^\circ.
\end{aligned} \tag{54}$$

It is easy to see that the most important theoretical uncertainty comes from the non-perturbative hadronic parameters, which can be improved later by the experiments.

At quark level, the decay channels related in this paper are all $b \rightarrow u$ transitions. This type of decays are suppressed by the CKM matrix elements, especially for the decays without a strange quark in the final states. This is one reason

TABLE III: Branching ratios of $B_{(s)} \rightarrow \bar{D}^* P$ decays calculated in PQCD approach together with experimental data [13](unit: 10^{-6}).

Modes	Class	Experiments	Our results
$\bar{B}^0 \rightarrow D_s^{*-} \pi^+$	T	30.0 ± 7.0	$41.7^{+21.9+2.5+4.1}_{-15.8-2.3-3.8}$
$\bar{B}^0 \rightarrow D_s^{*-} K^+$	E		$(0.36^{+0.10+0.16+0.04}_{-0.09-0.10-0.03}) \times 10^{-2}$
$\bar{B}^0 \rightarrow \bar{D}^{*0} \pi^0$	C		$(4.19^{+2.31+1.36+0.41}_{-1.61-1.16-0.39}) \times 10^{-2}$
$\bar{B}^0 \rightarrow \bar{D}^{*0} \bar{K}^0$	C		$2.35^{+1.2+0.94+0.23}_{-0.93-0.61-0.22}$
$\bar{B}^0 \rightarrow \bar{D}^{*0} \eta$	C		$(8.43^{+3.86+2.04+0.82}_{-2.94-1.86-0.78}) \times 10^{-2}$
$\bar{B}^0 \rightarrow \bar{D}^{*0} \eta'$	C		$(5.64^{+2.59+1.37+0.55}_{-1.97-1.26-0.53}) \times 10^{-2}$
$\bar{B}^0 \rightarrow D^{*-} \pi^+$	T		$1.21^{+0.67+0.08+0.12}_{-0.49-0.07-0.12}$
$B^- \rightarrow \bar{D}^{*0} \pi^-$	C		$(6.13^{+4.29+2.33+0.60}_{-3.17-1.84-0.57}) \times 10^{-2}$
$B^- \rightarrow \bar{D}^{*0} K^-$	C		$0.71^{+0.54+0.54+0.07}_{-0.36-0.39-0.07}$
$B^- \rightarrow D^{*-} \pi^0$	T	< 3.0	$0.65^{+0.36+0.05+0.06}_{-0.25-0.05-0.06}$
$B^- \rightarrow D^{*-} \bar{K}^0$	A	< 9.0	$1.46^{+0.44+0.04+0.14}_{-0.31-0.10-0.14}$
$B^- \rightarrow D^{*-} \eta$	T		$0.53^{+0.26+0.03+0.05}_{-0.19-0.05-0.05}$
$B^- \rightarrow D^{*-} \eta'$	T		$0.35^{+0.17+0.02+0.03}_{-0.13-0.03-0.03}$
$B^- \rightarrow D_s^{*-} \pi^0$	T		$22.7^{+12.2+1.4+2.3}_{-8.7-1.2-2.2}$
$B^- \rightarrow D_s^{*-} K^0$	A		$(6.95^{+2.00+0.97+0.68}_{-1.65-1.41-0.65}) \times 10^{-2}$
$B^- \rightarrow D_s^{*-} \eta$	T		$8.94^{+4.80+0.63+0.87}_{-3.56-0.93-0.83}$
$B^- \rightarrow D_s^{*-} \eta'$	T		$13.0^{+5.87+0.78+1.27}_{-4.42-0.79-1.21}$
$\bar{B}_s^0 \rightarrow \bar{D}^{*0} \pi^0$	E		$0.13^{+0.05+0.02+0.01}_{-0.04-0.02-0.01}$
$\bar{B}_s^0 \rightarrow \bar{D}^{*0} K^0$	C		$(3.25^{+1.9+1.9+0.3}_{-1.3-1.1-0.3}) \times 10^{-2}$
$\bar{B}_s^0 \rightarrow \bar{D}^{*0} \eta$	C		$1.16^{+0.57+0.21+0.11}_{-0.47-0.26-0.11}$
$\bar{B}_s^0 \rightarrow \bar{D}^{*0} \eta'$	C		$3.44^{+1.53+0.71+0.33}_{-1.25-0.71-0.32}$
$\bar{B}_s^0 \rightarrow D^{*-} \pi^+$	E		$0.27^{+0.09+0.04+0.03}_{-0.09-0.05-0.02}$
$\bar{B}_s^0 \rightarrow D^{*-} K^+$	T		$1.38^{+0.66+0.11+0.13}_{-0.50-0.16-0.13}$
$\bar{B}_s^0 \rightarrow D_s^{*-} K^+$	T		$36.2^{+18.7+3.4+3.8}_{-13.1-4.4-3.6}$

why most of the decays have small branching ratios with order 10^{-6} or 10^{-7} . Another reason is the absence of the color allowed emission diagrams with a light meson emitted.

As stated in previous section, all these decays do not have contributions from the penguin operators. For the tree operator induced decays, we have only four type of topology diagrams contributed: the color allowed diagrams (T), the color suppressed diagrams (C), the W annihilation decays (A) and the W exchange decays (E). All the decays are thus classified in the tables. From the numerical results, we can see that the pure annihilation type (“W” or “E”) decay branching ratios are suppressed comparing with the “T” or “C” emission diagrams dominant decay channels. Remember that the “T” and “C” emission diagrams dominant decay channels may also have “W” and “E” annihilation type contributions, although they are suppressed relatively. Within each category of decays, the large differences between channels are due to the Cabbibo suppression factor V_{cd}/V_{cs} .

Usually the nonfactorizable emission diagrams are suppressed comparing the factorizable diagrams. The two non-

TABLE IV: Predicted branching ratios of $B_{(s)} \rightarrow \bar{D}^* V$ decays(unit: 10^{-6}) and the percentage of transverse polarizations \mathcal{R}_T together with the experimental data[13].

Modes	Class	Experimental BRs	PQCD BRs	\mathcal{R}_T
$\bar{B}^0 \rightarrow D_s^{*-} \rho^+$	T		$68.2^{+33.9+4.49+6.65}_{-25.2-5.24-6.34}$	$(33^{+0.4+1.4}_{-0.4-1.3})\%$
$\bar{B}^0 \rightarrow D_s^{*-} K^{*+}$	E		$(1.91^{+0.44+0.43+0.19}_{-0.63-0.50-0.18}) \times 10^{-2}$	$(40^{+5.8+15.0}_{-0.0-6.9})\%$
$\bar{B}^0 \rightarrow \bar{D}^{*0} \rho^0$	C		$0.31^{+0.13+0.04+0.03}_{-0.11-0.05-0.03}$	$(84^{+1.4+2.6}_{-0.3-3.4})\%$
$\bar{B}^0 \rightarrow \bar{D}^{*0} \bar{K}^{*0}$	C	< 40	$13.5^{+6.20+1.76+1.32}_{-4.80-2.16-1.25}$	$(81^{+2.6+5.5}_{-0.6-4.5})\%$
$\bar{B}^0 \rightarrow \bar{D}^{*0} \omega$	C		$0.24^{+0.11+0.27+0.02}_{-0.09-0.04-0.02}$	$(72^{+0.0+4.4}_{-1.4-8.5})\%$
$\bar{B}^0 \rightarrow D^{*-} \rho^+$	T		$2.29^{+1.13+0.18+0.22}_{-0.86-0.17-0.21}$	$(34^{+0.0+1.3}_{-0.7-1.6})\%$
$B^- \rightarrow \bar{D}^{*0} \rho^-$	C		$1.10^{+0.42+0.15+0.11}_{-0.34-0.42-0.10}$	$(88^{+1.0+1.9}_{-2.1-3.3})\%$
$B^- \rightarrow \bar{D}^{*0} K^{*-}$	C		$26.1^{+9.93+3.68+2.54}_{-7.90-4.88-2.43}$	$(88^{+1.4+2.8}_{-1.1-3.0})\%$
$B^- \rightarrow D^{*-} \rho^0$	T		$1.50^{+0.70+0.11+0.15}_{-0.52-0.15-0.14}$	$(42^{+1.1+0.5}_{-1.5-1.5})\%$
$B^- \rightarrow D^{*-} \bar{K}^{*0}$	A		$2.25^{+0.68+0.26+0.22}_{-0.55-0.31-0.21}$	$(87^{+0.0+0.8}_{-2.2-3.0})\%$
$B^- \rightarrow D^{*-} \omega$	T		$1.01^{+0.52+0.07+0.10}_{-0.38-0.06-0.09}$	$(25^{+1.5+4.1}_{-1.5-4.0})\%$
$B^- \rightarrow D_s^{*-} \rho^0$	T		$36.8^{+18.2+2.41+3.59}_{-13.6-2.69-3.42}$	$(33^{+0.4+1.5}_{-0.4-1.4})\%$
$B^- \rightarrow D_s^{*-} K^{*0}$	A		$0.11^{+0.04+0.02+0.01}_{-0.02-0.03-0.01}$	$(89^{+1.4+0.18}_{-2.6-3.8})\%$
$B^- \rightarrow D_s^{*-} \omega$	T		$31.9^{+15.7+2.09+3.11}_{-11.8-2.42-2.97}$	$(33^{+0.4+1.4}_{-0.6-1.6})\%$
$B^- \rightarrow D_s^{*-} \phi$	A	< 12.0	$3.09^{+0.86+0.55+0.30}_{-0.73-0.77-0.29}$	$(89^{+0.8+0.9}_{-2.0-2.9})\%$
$\bar{B}_s^0 \rightarrow \bar{D}^{*0} \rho^0$	E		$0.17^{+0.05+0.04+0.02}_{-0.04-0.03-0.02}$	$(38^{+4.3+12.6}_{-3.4-7.2})\%$
$\bar{B}_s^0 \rightarrow \bar{D}^{*0} K^{*0}$	C		$0.49^{+0.21+0.09+0.05}_{-0.16-0.08-0.05}$	$(84^{+0.99+3.9}_{-1.7-5.5})\%$
$\bar{B}_s^0 \rightarrow \bar{D}^{*0} \omega$	E		$0.15^{+0.04+0.02+0.02}_{-0.04-0.02-0.01}$	$(37^{+4.0+13.3}_{-3.1-6.8})\%$
$\bar{B}_s^0 \rightarrow \bar{D}^{*0} \phi$	C		$11.7^{+4.89+1.88+1.15}_{-4.08-2.37-1.09}$	$(78^{+1.5+5.1}_{-0.2-4.6})\%$
$\bar{B}_s^0 \rightarrow D^{*-} \rho^+$	E		$0.34^{+0.10+0.06+0.03}_{-0.08-0.07-0.03}$	$(39^{+1.7+11.4}_{-2.4-8.1})\%$
$\bar{B}_s^0 \rightarrow D^{*-} K^{*+}$	T		$2.35^{+1.06+0.18+0.23}_{-0.81-0.23-0.22}$	$(32^{+0.1+1.3}_{-0.57-1.6})\%$
$\bar{B}_s^0 \rightarrow D_s^{*-} K^{*+}$	T		$64.8^{+29.6+5.57+6.32}_{-22.4-6.90-6.03}$	$(32^{+0.2-1.8}_{-0.2-1.5})\%$

factorizable diagrams in Fig.1(c,d) give nearly canceled contributions if the emitted meson is a light meson. However, it's not the situation here when the \bar{D} meson is emitted. \bar{c} quark and the light quark are very different in the emitted \bar{D} meson. As a result, the nonfactorizable emission diagrams also give non-negligible contributions. For example those channels with the $\bar{D}^{(*)0}$ meson in the final state are color suppressed. The Wilson coefficients for factorizable contribution ξ_{int} and nonfactorizable contribution \mathcal{M}_{int} are $a_2 = C_1 + C_2/3$ and $C_2/3$, respectively. Since $a_2 \approx C_2/3$, the $\xi_{int}(a_2)$ and $\mathcal{M}_{int}(C_2/3)$ give similar contributions. For these color suppressed modes, one can find that the annihilation diagrams can also give relatively large contributions. Our numerical results indicate that sometimes the annihilation diagrams' contributions do have the same order of magnitude as the emission diagrams. We also find that the twist-3 distribution amplitudes play an important role, especially in the annihilation diagrams.

When the charged $D^{(*)-}$ meson in the final state, the emission diagrams are the color favored ones, with the Wilson coefficients $a_1 = C_2 + C_1/3$ and $C_1/3$, for the factorizable diagrams and nonfactorizable diagrams, respectively. In this situation the nonfactorizable diagrams $\mathcal{M}_{int}(C_1/3)$ are highly suppressed by the Wilson coefficient, comparing with the factorizable diagrams $\xi_{int}(a_1)$, $\xi_{int}(a_1) \gg \mathcal{M}_{int}(C_1/3)$. This means that the dominant amplitudes with

$\xi_{int}(a_1)$ are nearly proportional to the product of $\bar{D}^{(*)}$ meson decay constant and a B to light meson form factor. This type of $B \rightarrow \bar{D}P$ decays have a little smaller branching ratios than those corresponding $B \rightarrow \bar{D}V$ decays, since the form factors of $B \rightarrow V$ are a little larger. However, in the color suppressed modes, $\xi_{int}(a_2) \sim \mathcal{M}_{int}(C_2/3)$, or pure annihilation type decays, the above conclusion is not satisfied. Because the large $\mathcal{M}_{int}(C_2/3)$ or the annihilation diagrams will bring more complicated situations. So the branching ratios of $B \rightarrow \bar{D}V$ are not definitely bigger than those of $B \rightarrow \bar{D}P$. From the Table I and II, we can see that some branching ratios of $B \rightarrow \bar{D}P$ are bigger than those of $B \rightarrow \bar{D}V$, which is different from $b \rightarrow c\bar{u}q$ decays.

For the $B_{(s)} \rightarrow \bar{D}_{(s)}^* V$ decays, we also calculate the ratio \mathcal{R}_T of the transverse polarization in the branching ratios, which is given by

$$\mathcal{R}_T = \frac{2(|\mathcal{A}^s|^2 + |\mathcal{A}^p|^2)}{|\mathcal{A}^N|^2 + 2(|\mathcal{A}^s|^2 + |\mathcal{A}^p|^2)}. \quad (55)$$

From Eq.(44)-Eq.(51), we can find that the transversely polarized contributions of the emission diagrams are suppressed by the factor r , and those of the W exchange diagrams are suppressed by the factor rr_V . That is the reason in category ‘‘T’’ and ‘‘E’’ decays, we have relatively small transverse polarization fractions.

For color suppressed emission diagrams (C), the factorizable contribution $\xi_{int}(a_2)$ and non-factorizable contribution $\mathcal{M}_{int}(C_2/3)$ are at the same order magnitude, none of which can give dominant contributions. The two diagrams of \mathcal{M}_{int} (longitudinal) cancel with each other and the two diagrams of \mathcal{M}_{int}^s and \mathcal{M}_{int}^p (transverse) strengthen with each other. So we can expect large transverse polarized contribution of the branching ratio. From table IV, we can see that all the ‘‘C’’ type decays have transverse polarization around 80%.

For the W exchange type decays, the factorizable annihilation contributions are suppressed by the Wilson coefficients, thus the dominant contribution is from nonfactorizable annihilation diagrams. One can find that the ratios of the transverse polarizations for the W exchange diagrams are around 40%. For the W annihilation type decays (A), the factorizable diagrams dominate the branching ratios due to the large Wilson coefficients. However, the two factorizable annihilation diagrams strongly cancel with each other in the longitudinally polarized case, while they strengthen with each other in transversely polarized cases. In addition, there is also cancelations between the factorizable and nonfactorizable contributions for the longitudinal polarizations. Therefore the transverse polarizations take a far more larger ratio in the branching ratios, which can be as large as nearly 90%.

The transverse polarization ratio do not depend on the variation of the CKM factors, since these kinds of overall factors cancel in the ratio. The uncertainty shown in table IV are from the hadronic uncertainty and factorization scale. Although these uncertainties are small, it does not mean that the polarization ratio is stable. In fact, it is quite sensitive to the hadronic wave function shape of the final state meson [14] and the power corrections.

$B^- \rightarrow D^0(\bar{D}^0)K^-$ decays can be used to measure γ angle, see Ref. [10], where the ratio $r \equiv \frac{|A(B^- \rightarrow \bar{D}^0 K^-)|}{|A(B^- \rightarrow D^0 K^-)|}$ is an important quantity. With the amplitudes we obtain, this ratio is given as

$$r = \frac{|A(B^- \rightarrow \bar{D}^0 K^-)|}{|A(B^- \rightarrow D^0 K^-)|} = 0.092_{-0.003}^{+0.012+0.003}. \quad (56)$$

The first error comes from the choice of the hard scales, and the second error comes from the CKM matrix elements. The uncertainty due to the hadronic parameters are canceled in the ratio, thus the calculation of the ratio is more precise and stable than the individual channels. With the formulas in Ref. [10], γ can be measured experimentally

through

$$R_i \equiv \frac{2[\Gamma(B^+ \rightarrow D_i K^+) + \Gamma(B^- \rightarrow D_i K^-)]}{\Gamma(B^+ \rightarrow \bar{D}^0 K^+) + \Gamma(B^- \rightarrow D^0 K^-)} = 1 + r^2 \pm \sqrt{4r^2 \cos^2 \gamma - \mathcal{A}^2 \cot^2 \gamma}, \quad (57)$$

where $i = 1, 2$, $D_{1,2} = (D^0 \pm \bar{D}^0)/\sqrt{2}$ corresponds to the two CP eigenstates, R_i is defined as two charge-averaged ratios for two CP eigenstates, and $\mathcal{A} = \mathcal{A}_2 - \mathcal{A}_1$ with

$$\mathcal{A}_i \equiv \frac{\Gamma(B^+ \rightarrow D_i K^+) - \Gamma(B^- \rightarrow D_i K^-)}{\Gamma(B^+ \rightarrow \bar{D}^0 K^+) + \Gamma(B^- \rightarrow D^0 K^-)}. \quad (58)$$

In Ref. [22], authors give similar diagrams on the relation of Eq. (57). One can find that the sensitivity of γ to the other quantities increases as the r decreases. When $r \sim 0.1$ the extracted γ will be very sensitive to \mathcal{A} . Thus our value of r may be too small for the current experiments.

IV. SUMMARY

In this paper, we investigate $B(B_s) \rightarrow \bar{D}_{(s)} P, \bar{D}_{(s)} V, \bar{D}_{(s)}^* P, \bar{D}_{(s)}^* V$ decays under the framework of perturbative QCD approach. We analyze the contributions of different diagrams in the leading order approximation of the m_D/m_B expansion. It is found that the nonfactorizable emission and annihilation diagram are also possible to give a large contribution. However, the emission contributions are still dominant in the branching ratios. All the branching ratios referred are calculated and the ratios of the transversely polarized contributions in the $B(B_s) \rightarrow \bar{D}_{(s)}^* V$ are also estimated. We find that the transversely polarized contributions, which mainly come from the nonfactorizable emission diagrams and annihilation type diagrams, are very large. In some channels, they are even dominant. The branching ratios of this kind of decays are around 10^{-6} and 10^{-7} , which means the method of extraction CKM angle γ is not effective in experiments.

Acknowledgements

This work is partly supported by National Natural Science Foundation of China under Grants No. 10735080, No. 10625525, and No. 10525523. We would like to thank W. Wang and Y.M. Wang for fruitful discussions.

APPENDIX A: WAVE FUNCTIONS AND DECAY CONSTANTS

1. Wave functions of $B_{(s)}$ mesons

The $B_{(s)}$ meson wave function are decomposed into the following Lorentz structures [15]

$$\begin{aligned} & \int \frac{d^4 z}{(2\pi)^4} e^{ik_1 \cdot z} \langle 0 | \bar{b}_\alpha(0) d_\beta(z) | B_{(s)}(P_1) \rangle \\ &= \frac{i}{\sqrt{2N_c}} \left\{ (P_1 + M_{B_{(s)}}) \gamma_5 [\phi_{B_{(s)}}(k_1) - \frac{\not{n} - \not{\bar{n}}}{\sqrt{2}} \bar{\phi}_{B_{(s)}}(k_1)] \right\}_{\beta\alpha}. \end{aligned} \quad (A1)$$

Here $\phi_{B_{(s)}}(k_1)$ and $\bar{\phi}_{B_{(s)}}(k_1)$ are the corresponding leading twist distribution amplitudes, and $\bar{\phi}_{B_{(s)}}(k_1)$ contributes little, so we neglect it. The final expression becomes

$$\Phi_{B_{(s)}} = \frac{i}{\sqrt{2N_c}} (P_1 + M_{B_{(s)}}) \gamma_5 \phi_{B_{(s)}}(k_1). \quad (A2)$$

The first determination of B-meson wave function was done in [16]. In our work the distribution amplitude in the b-space is a little differently:

$$\phi_{B(s)}(x, b) = N_{B(s)} x^2 (1-x)^2 \exp \left[-\frac{1}{2} \left(\frac{x M_{B(s)}}{\omega_b} \right)^2 - \frac{\omega_b^2 b^2}{2} \right], \quad (\text{A3})$$

Here b is the conjugate space coordinate of $\mathbf{k}_{1\perp}$. $N_{B(s)}$ is the normalization constant, which is determined by the normalization condition:

$$\int_0^1 dx \phi_{B(s)}(x, b=0) = \frac{f_{B(s)}}{2\sqrt{2}N_c}. \quad (\text{A4})$$

2. Wave functions and decay constants of light pseudoscalar mesons

The decay constant of the pseudoscalar meson is defined as:

$$\langle 0 | \bar{q}_1 \gamma_\mu \gamma_5 q_2 | P(P_3) \rangle = i f_P P_{3\mu}. \quad (\text{A5})$$

The Lorentz structure of light cone distribution amplitudes (for out-going state) for light pseudoscalar mesons is:

$$\begin{aligned} & \langle P(P_3) | q_{1\alpha}(0) \bar{q}_{2\beta}(z) | 0 \rangle \\ &= \frac{i}{\sqrt{2}N_c} \int_0^1 dx e^{ixP_3 \cdot z} \left[\gamma_5 \not{P} \phi^A(x) + \gamma_5 m_0 \phi^P(x) + m_0 \gamma_5 (\not{v} \not{n} - 1) \phi^T(x) \right]_{\alpha\beta}, \end{aligned} \quad (\text{A6})$$

where v is the light cone direction along which the light pseudoscalar meson's momentum is defined, and n is just opposite to it. The chiral scale parameter m_0 is defined as $m_0 = \frac{M_P^2}{m_{q_1} + m_{q_2}}$.

The distribution amplitudes are expanded by the Gegenbauer polynomials and their expressions are

$$\phi_P^A(x) = \frac{3f_P}{\sqrt{2}N_c} x(1-x) \left[1 + a_1^A C_1^{3/2}(t) + a_2^A C_2^{3/2}(t) + a_4^A C_4^{3/2}(t) \right], \quad (\text{A7})$$

$$\phi_P^p(x) = \frac{f_P}{2\sqrt{2}N_c} \left[1 + a_2^p C_2^{1/2}(t) + a_4^p C_4^{1/2}(t) \right], \quad (\text{A8})$$

$$\phi_P^T(x) = -\frac{f_P}{2\sqrt{2}N_c} \left[C_1^{1/2}(t) + a_3^T C_3^{1/2}(t) \right], \quad (\text{A9})$$

with $t = 2x - 1$. The coefficients of the Gegenbauer polynomials are [17]

$$\begin{aligned} a_{2\pi}^A &= 0.44, \quad a_{4\pi}^A = 0.25, \quad a_{1K}^A = 0.17, \quad a_{2K}^A = 0.2, \\ a_{2\pi}^p &= 0.43, \quad a_{4\pi}^p = 0.09, \quad a_{2K}^p = 0.24, \quad a_{4K}^p = -0.11, \\ a_{3\pi}^T &= 0.55, \quad a_{3K}^T = 0.35. \end{aligned} \quad (\text{A10})$$

The decay constants are

$$f_\pi = 131 \text{MeV}, \quad f_K = 160 \text{MeV}. \quad (\text{A11})$$

3. Wave functions and decay constants of light vector mesons

The decay constants for the vector mesons are defined by

$$\langle 0 | \bar{q}_1 \gamma_\mu q_2 | V(P_3, \epsilon) \rangle = f_V m_V \epsilon_\mu, \quad \langle 0 | \bar{q}_1 \sigma_{\mu\nu} q_2 | V(P_3, \epsilon) \rangle = i f_V^T (\epsilon_\mu P_{3\nu} - \epsilon_\nu P_{3\mu}). \quad (\text{A12})$$

Up to twist-3 the distribution amplitudes are

$$\begin{aligned}
\langle V(P_3, \epsilon_L^*) | q_{1\alpha}(0) \bar{q}_{2\beta}(z) | 0 \rangle &= -\frac{1}{\sqrt{2N_C}} \int_0^1 dx e^{ixP_3 \cdot z} [M_V \not{\epsilon}_L^* \phi_V(x) + \not{\epsilon}_L^* \not{P}_3 \phi_V^t(x) + M_V \phi_V^s(x)]_{\alpha\beta}, \\
\langle V(P_3, \epsilon_T^*) | q_{1\alpha}(0) \bar{q}_{2\beta}(z) | 0 \rangle &= -\frac{1}{\sqrt{2N_C}} \int_0^1 dx e^{ixP_3 \cdot z} [M_V \not{\epsilon}_T^* \phi_V^v(x) + \not{\epsilon}_T^* \not{P}_3 \phi_V^T(x) \\
&\quad + M_V i \epsilon_{\mu\nu\rho\sigma} \gamma_5 \gamma^\mu \epsilon_T^{*\nu} n^\rho v^\sigma \phi_V^a(x)]_{\alpha\beta},
\end{aligned} \tag{A13}$$

where x is the momentum fraction of the q_2 quark. Contrary to the pseudoscalar case, here n defines the light cone direction along which the momentum of light meson is taken and v is just the opposite light cone direction. The twist-2 distribution amplitudes of vector mesons are defined as

$$\begin{aligned}
\phi_V(x) &= \frac{3f_V}{\sqrt{2N_C}} x(1-x) [1 + a_1^\parallel C_1^{3/2}(t) + a_2^\parallel C_2^{3/2}(t)], \\
\phi_V^T(x) &= \frac{3f_V}{\sqrt{2N_C}} x(1-x) [1 + a_1^\perp C_1^{3/2}(t) + a_2^\perp C_2^{3/2}(t)].
\end{aligned} \tag{A14}$$

and the corresponding values of the Gegenbauer moments are [18]

$$\begin{aligned}
a_{2\rho}^\parallel &= a_{2\omega}^\parallel = 0.15 \pm 0.07, \quad a_{1K^*}^\parallel = 0.03 \pm 0.02, \quad a_{2K^*}^\parallel = 0.11 \pm 0.09, \quad a_{2\phi}^\parallel = 0.18 \pm 0.08, \\
a_{2\rho}^\perp &= a_{2\omega}^\perp = 0.14 \pm 0.06, \quad a_{1K^*}^\perp = 0.04 \pm 0.03, \quad a_{2K^*}^\perp = 0.10 \pm 0.08, \quad a_{2\phi}^\perp = 0.14 \pm 0.07.
\end{aligned} \tag{A15}$$

For the other distribution amplitudes, we use the asymptotic form

$$\begin{aligned}
\phi_V^t(x) &= \frac{3f_V^T}{2\sqrt{6}} t^2, \quad \phi_V^s(x) = \frac{3f_V^T}{2\sqrt{6}}(-t), \\
\phi_V^v(x) &= \frac{3f_V}{8\sqrt{6}}(1+t^2), \quad \phi_V^a(x) = \frac{3f_V}{4\sqrt{6}}(-t).
\end{aligned} \tag{A16}$$

The decay constants are listed below:

$$\begin{aligned}
f_\rho &= 209 \pm 2\text{MeV}, \quad f_{K^*} = 217 \pm 5\text{MeV}, \quad f_\omega = 195 \pm 3\text{MeV}, \quad f_\phi = 231 \pm 4\text{MeV}, \\
f_\rho^T &= 165 \pm 9\text{MeV}, \quad f_{K^*}^T = 185 \pm 10\text{MeV}, \quad f_\omega^T = 151 \pm 9\text{MeV}, \quad f_\phi^T = 186 \pm 9\text{MeV}.
\end{aligned} \tag{A17}$$

4. Wave function of $D^{(*)}$ meson

Up to twist-3 accuracy the two-particle light-cone distribution amplitudes of $D^{(*)}$ meson are defined as

$$\begin{aligned}
\langle D(P_2) | q_\alpha(z) \bar{c}_\beta(0) | 0 \rangle &= \frac{i}{\sqrt{2N_C}} \int_0^1 dx e^{ixP_2 \cdot z} [\gamma_5 (\not{P}_2 + M) \phi_D(x, b)]_{\alpha\beta} \\
\langle D^*(P_2) | q_\alpha(z) \bar{c}_\beta(0) | 0 \rangle &= -\frac{1}{\sqrt{2N_C}} \int_0^1 dx e^{ixP_2 \cdot z} [\not{\epsilon}_L (\not{P}_2 + M_{D^*}) \phi_{D^*}^L(x, b) + \not{\epsilon}_T (\not{P}_2 + M_{D^*}) \phi_{D^*}^T(x, b)]_{\alpha\beta}
\end{aligned} \tag{A18}$$

with

$$\int_0^1 dx \phi_D(x, 0) = \frac{f_D}{2\sqrt{2N_C}}, \quad \int_0^1 dx \phi_{D^*}^L(x, 0) = \frac{f_{D^*}}{2\sqrt{2N_C}}, \quad \int_0^1 dx \phi_{D^*}^T(x, 0) = \frac{f_{D^*}^T}{2\sqrt{2N_C}}, \tag{A19}$$

as the normalization conditions. In the heavy quark limit we have

$$f_{D^*}^T - f_{D^*} \frac{m_c + m_d}{M_{D^*}} \sim f_{D^*} - f_{D^*}^T \frac{m_c + m_d}{M_{D^*}} \sim O(\bar{\Lambda}/M_{D^*}). \tag{A20}$$

Thus we will use $f_{D^*}^T = f_{D^*}$ in our calculation. The models for the distribution amplitude for D meson we used in this paper is

$$\phi_D^{(MGen)}(x, b) = \frac{1}{2\sqrt{2N_c}} f_D 6x(1-x)[1 + C_D(1-2x)] \exp\left[\frac{-\omega^2 b^2}{2}\right]. \quad (\text{A21})$$

The masses of $D_{(s)}^{(*)}$ meson we use are

$$\begin{aligned} m_D &= 1.869\text{GeV}, & m_{D_s^-} &= 1.968\text{GeV}, \\ m_{D^*} &= 2.010\text{GeV}, & m_{D_s^{*-}} &= 2.112\text{GeV}. \end{aligned} \quad (\text{A22})$$

We take $f_D = 207\text{MeV}$ [19], $C_D = 0.5$, $\omega = 0.1\text{GeV}$ for \bar{D} meson, $f_{D_s} = 241\text{MeV}$ [19], $C_D = 0.4$, $\omega = 0.3\text{GeV}$ for \bar{D}_s meson. We use the relations between f_D and f_{D^*} derived from HQET [20]:

$$f_{D^*} = \sqrt{\frac{m_D}{m_{D^*}}} f_D, \quad f_{D_s^{*-}} = \sqrt{\frac{m_{D_s^-}}{m_{D_s^{*-}}}} f_{D_s^-}. \quad (\text{A23})$$

APPENDIX B: PQCD FUNCTIONS

The pQCD functions appear in (7)-(10) and (44)-(51) are listed as

$$\begin{aligned} h_i(x_1, x_2, b_1, b_2) &= K_0(\sqrt{x_1 x_2} m_B b_1) \\ &\times [\theta(b_1 - b_2) K_0(\sqrt{x_2} m_B b_1) I_0(\sqrt{x_2} m_B b_2) \\ &+ \theta(b_2 - b_1) K_0(\sqrt{x_2} m_B b_2) I_0(\sqrt{x_2} m_B b_1)], \end{aligned} \quad (\text{B1})$$

$$\begin{aligned} h_a(x_2, x_3, b_2, b_3) &= \left(i\frac{\pi}{2}\right)^2 H_0^{(1)}(\sqrt{x_2 x_3} m_B b_2) \\ &\times \left[\theta(b_2 - b_3) H_0^{(1)}(\sqrt{x_3} m_B b_2) J_0(\sqrt{x_3} m_B b_3) \right. \\ &\left. + \theta(b_3 - b_2) H_0^{(1)}(\sqrt{x_3} m_B b_3) J_0(\sqrt{x_3} m_B b_2)\right], \end{aligned} \quad (\text{B2})$$

where $H^{(1)}(z) = J_0(z) + iY_0(z)$. And

$$\begin{aligned} h_d^{(j)} &= [\theta(b_1 - b_2) K_0(D m_B b_1) I_0(D m_B b_2) + \theta(b_2 - b_1) K_0(D m_B b_2) I_0(D m_B b_1)] \\ &\times \left\{ \begin{array}{l} K_0(D_j m_B b_2) \quad \text{for } D_j^2 \geq 0 \\ \frac{i\pi}{2} H_0^{(1)}(\sqrt{|D_j^2|} m_B b_2) \quad \text{for } D_j^2 \leq 0 \end{array} \right\}, \end{aligned} \quad (\text{B3})$$

$$\begin{aligned} h_f^{(j)} &= i\frac{\pi}{2} \left[\theta(b_1 - b_2) H_0^{(1)}(F m_B b_1) J_0(F m_B b_2) + \theta(b_2 - b_1) H_0^{(1)}(F m_B b_2) J_0(F m_B b_1) \right] \\ &\times \left\{ \begin{array}{l} K_0(F_j m_B b_1) \quad \text{for } F_j^2 \geq 0 \\ \frac{i\pi}{2} H_0^{(1)}(\sqrt{|F_j^2|} m_B b_1) \quad \text{for } F_j^2 \leq 0 \end{array} \right\}, \end{aligned} \quad (\text{B4})$$

with the variables

$$\begin{aligned} D^2 &= x_1(1-x_3)(1-r^2), \\ D_1^2 &= (x_1-x_2)(1-x_3)(1-r^2), \\ D_2^2 &= (x_1+x_2)r^2 - (1-x_1-x_2)(1-x_3)(1-r^2), \\ F^2 &= x_2(1-x_3)(1-r^2), \\ F_1^2 &= 1 - (1-x_2)(1-x_1 - (1-x_3)(1-r^2)), \\ F_2^2 &= x_2(x_1 - (1-x_3)(1-r^2)). \end{aligned} \quad (\text{B5})$$

The hard scales are determined by

$$\begin{aligned}
t_i^{(1)} &= \max(\sqrt{(1-x_3)(1-r^2)}m_B, 1/b_1, 1/b_3), & t_i^{(2)} &= \max(\sqrt{x_1(1-r^2)}m_B, 1/b_1, 1/b_3), \\
t_a^{(1)} &= \max(\sqrt{x_2(1-r^2)}m_B, 1/b_2, 1/b_3), & t_a^{(2)} &= \max(\sqrt{(1-x_3)(1-r^2)}m_B, 1/b_2, 1/b_3), \\
t_d^{(j)} &= \max(Dm_B, \sqrt{|D_j^2|}m_B, 1/b_1, 1/b_2), & t_f^{(j)} &= \max(Fm_B, \sqrt{|F_j^2|}m_B, 1/b_1, 1/b_2).
\end{aligned} \tag{B6}$$

Jet function appears in the factorization formulae is

$$S_t(x) = \frac{2^{1+2c} \Gamma(3/2 + c)}{\sqrt{\pi} \Gamma(1 + c)} [x(1-x)]^c, \tag{B7}$$

with $c = 0.5$ in this paper.

The expressions for the functions $E_l(t)$, with $l = i, a, d, f$, are

$$\begin{aligned}
E_i(t) &= \alpha_s(t) \exp[-S_B(t) - S_3(t)], \\
E_a(t) &= \alpha_s(t) \exp[-S_D(t) - S_3(t)], \\
E_d(t) &= \alpha_s(t) \exp[-S(t)|_{b_3=b_1}], \\
E_f(t) &= \alpha_s(t) \exp[-S(t)|_{b_3=b_2}],
\end{aligned} \tag{B8}$$

where the Sudakov exponent $S = S_B + S_D + S_3$, with S_3 as the Sudakov exponent of the light meson. And the $S_j(x_i)(j = B, D$ or $3)$ functions in Sudakov form factors are

$$S_B(t) = s\left(x_1 \frac{m_B}{\sqrt{2}}, b_1\right) + 2 \int_{1/b_1}^t \frac{d\bar{\mu}}{\bar{\mu}} \gamma_q(\alpha_s(\bar{\mu})), \tag{B9}$$

$$S_D(t) = s\left(x_2 \frac{m_B}{\sqrt{2}}, b_2\right) + 2 \int_{1/b_2}^t \frac{d\bar{\mu}}{\bar{\mu}} \gamma_q(\alpha_s(\bar{\mu})), \tag{B10}$$

$$S_3(t) = s\left(x_3 \frac{m_B}{\sqrt{2}}, b_3\right) + s\left((1-x_3) \frac{m_B}{\sqrt{2}}, b_3\right) + 2 \int_{1/b_3}^t \frac{d\bar{\mu}}{\bar{\mu}} \gamma_q(\alpha_s(\bar{\mu})), \tag{B11}$$

with the quark anomalous dimension $\gamma_q = -\alpha_s/\pi$. The explicit form for the function $s(Q, b)$ is:

$$\begin{aligned}
s(Q, b) &= \frac{A^{(1)}}{2\beta_1} \hat{q} \ln\left(\frac{\hat{q}}{\hat{b}}\right) - \frac{A^{(1)}}{2\beta_1} (\hat{q} - \hat{b}) + \frac{A^{(2)}}{4\beta_1^2} \left(\frac{\hat{q}}{\hat{b}} - 1\right) - \left[\frac{A^{(2)}}{4\beta_1^2} - \frac{A^{(1)}}{4\beta_1} \ln\left(\frac{e^{2\gamma_E} - 1}{2}\right)\right] \ln\left(\frac{\hat{q}}{\hat{b}}\right) \\
&+ \frac{A^{(1)}\beta_2}{4\beta_1^3} \hat{q} \left[\frac{\ln(2\hat{q}) + 1}{\hat{q}} - \frac{\ln(2\hat{b}) + 1}{\hat{b}}\right] + \frac{A^{(1)}\beta_2}{8\beta_1^3} [\ln^2(2\hat{q}) - \ln^2(2\hat{b})],
\end{aligned} \tag{B12}$$

where the variables are defined by

$$\hat{q} \equiv \ln[Q/(\sqrt{2}\Lambda)], \quad \hat{b} \equiv \ln[1/(b\Lambda)], \tag{B13}$$

and the coefficients $A^{(i)}$ and β_i are

$$\begin{aligned}
\beta_1 &= \frac{33 - 2n_f}{12}, \quad \beta_2 = \frac{153 - 19n_f}{24}, \\
A^{(1)} &= \frac{4}{3}, \quad A^{(2)} = \frac{67}{9} - \frac{\pi^2}{3} - \frac{10}{27}n_f + \frac{8}{3}\beta_1 \ln\left(\frac{1}{2}e^{\gamma_E}\right),
\end{aligned} \tag{B14}$$

n_f is the number of the quark flavors and γ_E is the Euler constant. We will use the one-loop running coupling

constant, i.e. we pick up the four terms in the first line of the expression for the function $s(Q, b)$.

-
- [1] M.Beneke, G.Buchalla, M.Neubert and C.T. Sachrajda, Phys. Rev. Lett. 83, 1914(1999)[hep-ph/9905312]; Nucl. Phys. B591, 313 (2000)[hep-ph/0006124].
- [2] C.W.Bauer, D. Pirjol, I.W.Stewart, Phys. Rev. Lett. 87(2001) 201806 [hep-ph/0107002]; Phys. Rev. D65,054022 (2002) [hep-ph/0109045].
- [3] Y.Y.Keum, H.-n. Li and A.I.Sanda, Phys. Lett. B504,6(2001) [hep-ph/004004]; Phys. Rev. D63,054008 (2001)[hep-ph/0004173]; C.D.-Lu, K. Ukai and M.-Z.Yang, Phys. Rev. D63, 074009(2001) [hep-ph/0109045]; C.D.-Lu and M.-Z.Yang, Eur. Phys. J. C23, 275-287 (2002) e-Print: hep-ph/0011238.
- [4] M. A. Shifman, A. I. Vainshtein and V. I. Zakharov, Nucl. Phys. B **147**, 385 (1979); L. J. Reinders, H. Rubinstein and S. Yazaki, Phys. Rept. **127**, 1 (1985); P. Colangelo and A. Khodjamirian. arXiv:hep-ph/0010175.
- [5] I. I. Balitsky, V. M. Braun and A. V. Kolesnichenko, Nucl. Phys. B **312**, 509 (1989).
- [6] M. Gronau and D. London, Phys. Lett. B **253**, 483 (1991); M. Gronau and D. Wyler, Phys. Lett. B **265**, 172 (1991).
- [7] H. n. Li, Phys. Rev. D **52**, 3958 (1995) [arXiv:hep-ph/9412340]; C. Y. Wu, T. W. Yeh and H. n. Li, Phys. Rev. D **53**, 4982 (1996) [arXiv:hep-ph/9510313]; Y.Y. Keum et al., Phys. Rev. D69, 094018 (2004) e-Print: hep-ph/0305335; C.D. Lu, Phys. Rev. D68, 097502 (2003) [arXiv:hep-ph/0307040].
- [8] C.D. Lu, Eur. Phys. J. C24, 121-126 (2002) e-Print: hep-ph/0112127; Y. Li and C.D. Lu, High Energy Phys. Nucl. Phys. 27, 1062-1066 (2003) e-Print: hep-ph/0305278; J. F. Cheng, D. S. Du and C. D. Lu, Eur. Phys. J. C **45**, 711 (2006) [arXiv:hep-ph/0501082].
- [9] R.H. Li, C.D. Lü, H. Zou, Phys. Rev. D 78, 014018 (2008).
- [10] M. Gronau, Phys. Rev. D **58**, 037301 (1998) [arXiv:hep-ph/9802315].
- [11] B.-H. Hong, C.-D. Lu, Sci. China G49, 357-366 (2006) e-Print: hep-ph/0505020
- [12] T. Feldmann, P. Kroll and B. Stech, Phys. Rev. D **58**, 114006 (1998) [arXiv:hep-ph/9802409]; T. Feldmann, P. Kroll and B. Stech, Phys. Lett. B **449**, 339 (1999) [arXiv:hep-ph/9812269].
- [13] C. Amsler et al. (Particle Data Group), Physics Letters B667, 1 (2008).
- [14] A. L. Kagan, Phys. Lett. B601, 151-163 (2004) e-Print: hep-ph/0405134; H.-n. Li, Phys. Lett. B622, 63-68 (2005) e-Print: hep-ph/0411305; Y. Li, C.-D. Lu, Phys. Rev. D73, 014024 (2006) e-Print: hep-ph/0508032; H.W. Huang, et al., Phys. Rev. D73, 014011 (2006) e-Print: hep-ph/0508080
- [15] A. G. Grozin and M. Neubert, Phys. Rev. D **55**, 272 (1997) [arXiv:hep-ph/9607366]; H. Kawamura, J. Kodaira, C.-F. Qiao, K. Tanaka, Phys. Lett. B523, 111 (2001); Erratum-ibid. B536, 344 (2002) e-Print: hep-ph/0109181; Mod. Phys. Lett. A18, 799 (2003) e-Print: hep-ph/0112174; H. n. Li and H. S. Liao, Phys. Rev. D **70**, 074030 (2004) [arXiv:hep-ph/0404050].
- [16] H. n. Li and B. Melic, Eur. Phys. J. C **11**, 695 (1999) [arXiv:hep-ph/9902205].
- [17] V. L. Chernyak and A.R. Zhitnitsky, Phys. Rept. **112**, 173 (1984); V. M. Braun and I. E. Filyanov, Z. Physik C**44**, 157 (1989); P. Ball, JHEP **9809**, 005 (1998) [hep-ph/9802394]; V. M. Braun and I. E. Filyanov, Z. Physik C**48**, 239 (1990); A. R. Zhitnitsky, I. R. Zhitnitsky and V. L. Chernyak, Sov. J. Nucl. Phys. **41**, 284(1985), Yad. Fiz. **41**, 445 (1985).
- [18] P. Ball and R. Zwicky, Phys. Rev. D **71**, 014029 (2005); P. Ball and R. Zwicky, JHEP **0604**, 046 (2006); JHEP **0703**, 069 (2007).
- [19] E. Follana, C. T. H. Davies, G. P. Lepage and J. Shigemitsu [HPQCD Collaboration and UKQCD Collaboration], Phys. Rev. Lett. **100**, 062002 (2008) [arXiv:0706.1726 [hep-lat]].
- [20] A. V. Manohar and M. B. Wise, Camb. Monogr. Part. Phys. Nucl. Phys. Cosmol. **10**, 1 (2000).
- [21] D. Atwood, I. Dunietz, and A. Soni, Phys. Rev. Lett. **78**,3257(1997); see also N. Sinha and R. Sinha, Phys. Rev. Lett.

80,3706(1998).

- [22] M. Gronau and J. L. Rosner, Phys. Rev. D **57**,6843(1998). Here R , A_0 , r and γ , defined in an analogous way for $B \rightarrow K\pi$, obey the same relation as R_i , \mathcal{A} , r , and γ in $B \rightarrow DK$.